Article

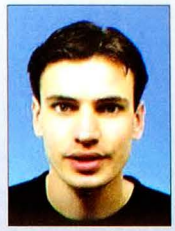

# Survey Plan Improvement by Detecting Sea Floor Dynamics in Archived Echo Sounder Surveys

By Leendert L. Dorst, Hydrographic Service of the Royal Netherlands Navy, The Netherlands and Water Engineering and Management, University of Twente, The Netherlands

**Abstract**

*The publication of up-to-date nautical charts of shallow seas requires periodic resurveys. Information on the behaviour of the sea floor improves the planning of resurvey frequencies, which could be provided by an analysis of a series of archived sea floor surveys. We present a method to extract those dynamics using deformation analysis. It models a sloping plane for a limited area of the sea floor. The method judges whether differences between surveys are statistically significant with respect to the survey accuracy. This way, different kinds of sea floor behaviour can be detected, and the detected deformations are estimated. The procedure is illustrated by an anexample in the southern North Sea.*

**Résumé**

*La publication de cartes à jour de mers peu profondes nécessite l'exécution de nouveaux levés périodiques. Les informations sur le comportement du fond de la mer permettent d'améliorer la planification des fréquences d'exécution des nouveaux levés, laquelle pourrait être assurée par l'analyse d'une série de levés du fond archivée. Nous présentons une méthode qui permet d'extraire ces dynamiques en utilisant l'analyse des déformations. Il s'agit de la modélisation d'un plan incliné pour une zone limitée du fond. La méthode permet de juger si les différences entre les levés sont statistiquement importantes du point de vue de la précision du levé. C'est ainsi que différentes sortes de comportement du fond de la mer peuvent être détectées et que les dimensions des déformations détectées et que les déformations détectées sont estimées. Cette procédure est illustrée à l'aide d'un exemple concernant la mer du Nord.*

**Resumen**

*La publicación de cartas actualizadas requiere nuevos levantamientos periódicos. La información sobre el comportamiento del fondo marino mejora la planificación de las frecuencias de los nuevos levantamientos, lo que puede lograrse mediante el análisis de una serie de levantamientos de archivo del fondo submarino. Presentamos aquí un método para obtener esa dinámica, utilizando análisis de deformación, que modelan una superficie en pendiente para un área limitada del fondo submarino. Este método determina si las diferencias entre levantamientos tienen importancia estadística con respecto a la precisión del levantamiento. De esta manera se podrán detectar diferentes tipos de comportamiento del fondo submarino y así calcular las deformaciones detectadas. El procedimiento se ilustra con un ejemplo en el Mar del Norte.*

## 1. Introduction

The North Sea has a dynamic sea floor, that shows sand wave patterns at various scales [e.g. Nemeth et al., 2002]. Therefore, the depth information in nautical charts should be updated with new surveys regularly. The Hydrographic Service of the Royal Netherlands Navy uses a survey plan, that describes the aimed resurvey frequency for the Netherlands Continental Shelf. Shallow areas, as well as areas with intense traffic, are surveyed more frequently than the other areas. In an attempt to deploy its two new multi-beam survey vessels, HNLMS *Snellius* and *Luymes*, more efficiently, the Hydrographic Office quests for information on the kind and size of sea floor evolution.

Information on sea floor evolution could be obtained from physical models for natural evolution [e.g. Nemeth et al., 2002] and human intervention [e.g. Roos and Hulscher, 2003], or from the analysis of a time series of depth data, like echo sounder surveys. Several techniques for sea floor data analysis have been proposed, for instance by Wright [1992], who observes the evolution of sand wave crests in the southern North Sea. A second data analysis example is the observation of regeneration of sand waves after dredging, by Knaapen and Hulscher [2002]. A recent example of the time analysis of river bed data is the work of Sieben [2004]; he concentrates on the dynamic modelling of spatial bed fluctuations. However, the stochastic character of measured data sets has not been taken into account in those analyses.
The quantification of uncertainty in bathymetric data is a field of growing interest, as recent publications show [e.g. Calder, 2003; Smith et al., 2002]. This stochastic character complicates the analysis of bed evolution: survey equipment measures depths with a limited accuracy, like any other measurement process. The required accuracies for hydrographic surveys has been defined in the S44 standard [International Hydrographic Organization, 1998; Wells and Monahan, 2002]. The interpretation of any time series of data has to answer the question which observed differences are due to real changes, and when they should be explained by inaccuracies of the data collection process.

Wüst [2004] analyses local trends in series of depth data by an elegant method that is aware of the stochastic properties of depth data. However, the desired analysis method for survey plan improvement can distinguish between different kinds of dynamics: it can distinguish between general sea floor shoaling and growth of the sand waves, identify an outlying survey, separate clear trends from a static situation, and recognise true sea floor deformation in noisy data.
This article presents deformation analysis as a method for survey analysis in the presence of observation noise, in combination with variance propagation and geostatistical interpolation. "Deformation analysis" refers to the application of statistical testing theory to a time series of surveys [Caspary, 1987]. Also, it shows the method is suitable to support decisions about resurvey frequencies. Menting [2004] compares the presented method to the one proposed by Wüst [2004].

The structure of the article is as follows (Figure 1): first, details about an example on the Netherlands Continental Shelf are provided. The example shows the analysis of six surveys of this heavily surveyed area for illustrative purposes. Then, every step of the proposed method is treated in its own section:

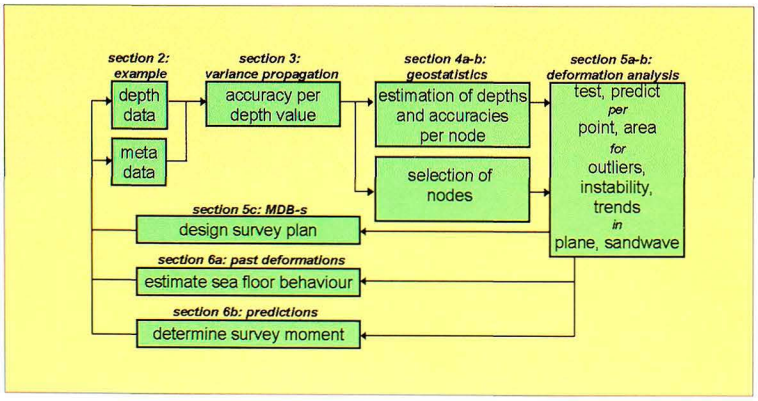


*Figure 1:The developed method uses depth data from echo sounders and their survey characteristics ("meta data") to calculate firstly the accuracy of every depth value, then depth values and their accuracies at a set of grid nodes, and finally it analyses those grids in time. The method can be applied in several ways to improve the survey plan, which influences the collection of depth data and their meta data*

variance propagation, geostatistics and deformation analysis. For each step, a method section gives insight into the followed procedure, without giving a full mathematical treatment, and then we present the results for the example. The mathematical details of this application of deformation analysis will be given in Dorst [2005]. The results of the last step are given in a separate section, section 6. Figure 1 also shows the feedback possibilities to the collection of data, through adaptations in the survey plan. Section 7 critically discusses the method and the three feedback possibilities. Finally, some conclusions are drawn in section 8.

## 2. A North Sea Example

The steps of the presented method are illustrated by the archived surveys of a small area of the Netherlands Continental Shelf. The example is a part of the "selected track" to the port of Rotterdam (Figure 2). The selected track is the approach route for large ships that navigate through the Channel. At some places along this track, depth under mean lower low water spring level is less than thirty metres, mostly due to the presence of sand banks and sand waves. We follow the terminology of Knaapen et al. [2001] for spatially rhythmic features of the sea floor. The sand banks have a width of several kilometres, the sand waves several hundreds of metres. Around these shallow parts, eleven critical areas have been defined.

Figure 2 shows the selected track and its "critical areas". Those areas are not dredged, but frequently monitored by the Royal Netherlands Navy hydrographic ships. The Southern part of "critical area I" is taken as an example here; it has been surveyed six times since 1991. The critical area was placed around a shallow structure, which shows larger dynamics than most of the other critical areas. Other examples of analysed critical areas are available as well [Dorst, 2004a and 2004b]. A recent description of the physical properties of the sea floor in this region has been given by Hulscher and Van den Brink [2001].

A Matlab toolbox, developed by the author, has performed the calculations and visualisations of the example. The example was analysed using Matlab 6.5, including the optimisation and statistics toolboxes. For the interpolation, use was made of the Kriging toolbox of Gratton, from the University of Quebec [www.inrs-eau.uquebec.ca/activites/repertoire/profs/yg/krig.htm]. It contains the functions of Deutsch and Journel [1992] and of Marcotte [1991].

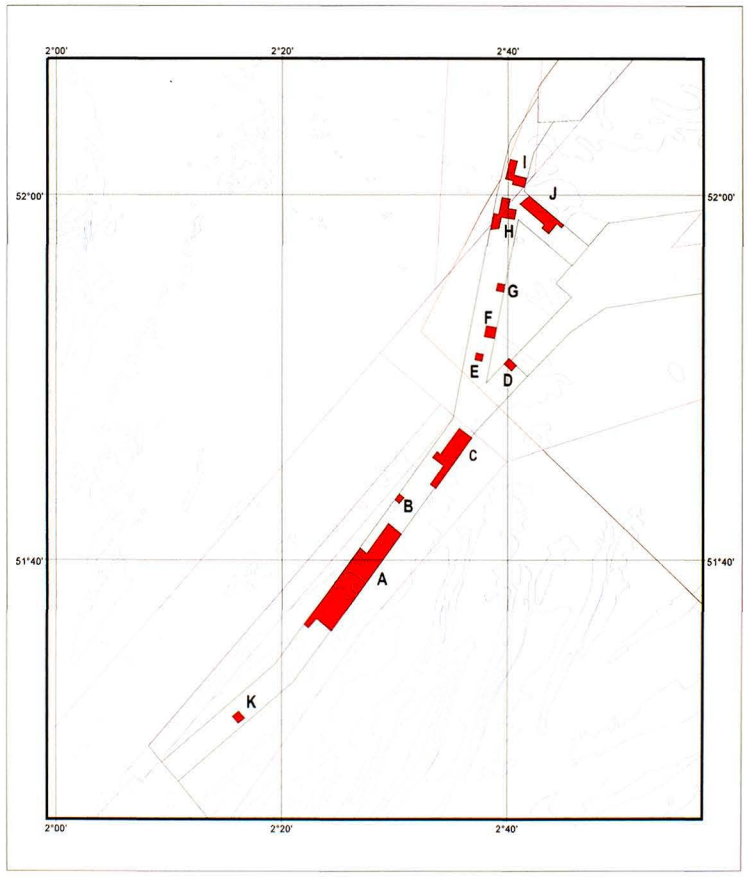


*Figure 2: The selected track (black lines) and its critical areas (red areas). Also, the figure shows the 30-metre depth line under mean lower low water spring level (blue lines), the traffic separation scheme (magenta lines) and the limit of the Netherlands territorial sea (orange line). (Figure courtesy of A. Visser, Hydrographic Service of the Royal Netherlands Navy)*

## 3. Variance Propagation

The first step of the method is to quantify the propagation [Teunissen, 2000] of all the stochastic infuences on depth measurement, i.e. to determine an accuracy indication for every sounding. Such an *a priori* estimation of variances requires "meta data", which describe the survey: tidal reduction technique, positioning method, etc. All aspects of the survey process need to be taken into account, which makes this a rather complex task. For instance, the Royal Navy has a model for variance propagation in hydrography [Hydrographic Department, 1990]. Alternatively, *a posteriori* variance estimates could be used, obtained by the binning of soundings. Such variance estimations usually give accuracies that are too small, due to the spatial and temporal correlations in depth measurements [Smith et al, 2002].

Table 1 quantifies the stochastic influences of the 2003 survey of critical area I. All accuracies are according to the specifications of the instruments. Some depend on the measured depth $\underline{d}$. The effect of sound velocity measurement on depth depends on the propagation speed of sound through water, which we assume *1500m/s* [Schaap, 2000]. The given dynamic draft accuracy has been studied by Elema and Kwanten [1999]. Versteeg [2000] gives details about the tidal reduction. Information on the sea state (mean heave amplitude $\bar{h}$) and the sea floor variability (mean slope $\bar{\alpha}$) has to be included as well. Cressie and Kornak [2003] introduce a more sophisticated method to determine the influence of positioning accuracy on depth accuracy. Their algorithm will be studied, and might replace the current inclusion of positioning accuracy.

When a survey ship experiences too large rotations, the crew aborts the survey. Small ship rotations are compensated by the echo sounder beam width. The idealisation precision of the sea floor includes the early reflection of the beam from a closer point than the one directly under the ship, and the presence of small-scale variations like ripples and megaripples. Those effects on the measured depths are neglected, although they might lead to a worse accuracy. Also, post-processing effects like shoal-biasing make the accuracy worse. It should thus be kept in mind that the true accuracy may be worse than specified. Therefore, the total propagated accuracy of an observed depth value $1.96\sigma_d$ is modelled at 95% probability as:

$$\sqrt{\sum_i (1.96\sigma_i)^2}\,\text{m}. \qquad (1)$$

## 4a. Geostatistics: Theory

Interpolation is necessary to obtain gridded depth data, unless a survey fully covers the sea floor. Geostatistics [Chilès and Delfiner, 1999] is used here for this task, which is the second step of the method. It can calculate the resulting accuracies of the interpolated depths. Hereto, the spatial variability of the sea floor is described by a covariance function. It describes the expected similarity between data points as a function of distance and direction. The covariance function can be calculated from a set of survey data that all show the same spatial sea floor behaviour. It can consecutively be used for the determination of interpolation weights. Interpolating with these weights is called kriging.

| stochastic influence | effect on depth accuracy, at 95% [$m$] |
|---|---|
| echo sounder ($1.96\sigma_1$) | $0.002 \cdot \underline{d} + 0.05$ |
| sound velocity measurement ($1.96\sigma_2$) | $\underline{d}/3000$ |
| heave sensor ($1.96\sigma_3$) | $0.2 \cdot \bar{h}$ |
| static draft measurement ($1.96\sigma_4$) | 0.05 |
| dynamic draft measurement ($1.96\sigma_5$) | 0.03 |
| tidal reduction ($1.96\sigma_6$) | 0.2 |
| horizontal accuracy, DGPS ($1.96\sigma_7$) | $(\bar{\alpha}/100\%) \cdot 5$ |
| roll and pitch measurement | neglected |
| sea floor idealisation | neglected |

*Table 1: Sources of noise for the surveys of critical area I, and their influence on the depth accuracy. This makes the total propagated accuracy a function of depth $\underline{d}$, mean heave $\bar{h}$ and mean slope $\bar{\alpha}$. All surveys were performed by the Royal Netherlands Navy survey ships between 1991 and 2003, using single-beam echo sounders. Sound velocity was measured with 2m/s accuracy, at 95%; the horizontal DGPS accuracy is assumed 5m, at 95%*

Kriging is useful to obtain both depths and variances for the nodes of the grid, especially if the sea floor is relatively smooth. A smooth sea floor implies a high correlation over large distances, and therefore node depths can be estimated accurately from the surveyed depths.

Kriging has been applied to the sea floor several times before [Kielland and Dagbert, 1992; Velberg, 1993]. Here, for instance a sand dune requires anisotropic estimation. The direction of the highest variability is chosen as the x-direction. In case of sand waves, this corresponds to the direction perpendicular to the wave crests. This is often also the direction of the survey tracks. It could also be estimated, e.g. by the DIGIPOL algorithm [RIKZ, 1997]. We propose a modified version of this algorithm:

1. Remove the trend from an area
2. Grid the data to a dense grid, and do not mind about nodes without data
3. Calculate gradients in both the grid directions, for the nodes where this is possible
4. Average the gradients to two mean absolute values, for the two grid directions
5. The direction of highest variability is the tangent of the quotient of these directions
6. Check the results: the correct direction could also be *360°* minus the found azimuth, and single-beam surveys often give biased results to the track direction.

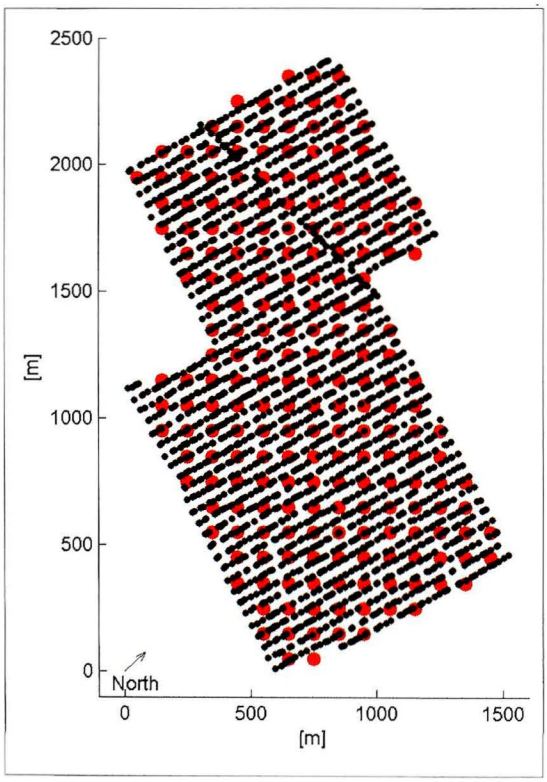


*Figure 3: Surveyed positions (small black dots) and interpolation nodes (large red nodes), for the 2003 survey of the Southern part of critical area I. The horizontal axis of the grid points in the direction x, which is the direction of highest variability. The perpendicular axis y consequently has the lowest variability*

The covariance function is calculated by finding autocovariances between distance intervals in the perpendicular horizontal directions *x* and *y*. Direction *x* is the direction of highest spatial variability; *y* consequently has the lowest variability. In the absence of sand waves a gaussian function often fits well through the calculated autocovariance values:

$$c(h) = b?e^{-(h/a)^2} + d\,. \qquad (2)$$

Here, *h* is the distance, and the parameters *a*, *b*, and *d* represent the "range", the "sill" and the "nugget" respectively [Chilès and Delfiner, 1999]. When the sea floor is isotropic, i.e. its characteristics are direction independent, the estimation of a single gaussian function through omnidirectional autocovariance values suffices. In all other cases, the two functions are combined to a single two-dimensional function by:

$$c(h_x, h_y) = c_x(h_x) \cdot c_y(h_y) / c(0), \qquad (3)$$

where $h_x$ and hy are the distances in the directions *x* and *y*. If sand waves are present, a cosine factor is added to $c_x(h_x)$. $c(0)$ is a singular value of both the functions that represents the variance at a position *(x,y)*. Here, $\sigma_d^2$ is valid, cf. equation (1).

The grid is oriented in the x-direction. The node distance should be small enough to avoid aliasing effects of the relevant structures on the sea floor. On the other hand, a high node density leads to a high computational effort. Moreover, close nodes have a high correlation, which we neglect in the next step, for computational reasons. Very close nodes are therefore undesirable. Experience shows that a good choice for the node density is often twice the survey spacing. The kind of kriging that is applied here is ordinary point kriging. [Chilès and Delfiner, 1999] It estimates the inter-

polation weights from the covariance values between the observed positions and the node, such that the sum of the weights equals one. The omission of remote observations makes the computation faster, without a lot of influence on the nodal depths. Actually, it decreases the covariance between the nodes, which is undesirable in the deformation analysis.

### 4b. Geostatistics: The Example

Figure 3 shows the survey tracks and the defined grid for the example. The direction of highest variability has an azimuth of *41°*, which was estimated by the proposed algorithm. The grid distance is *100m*. The used survey depths are the shallowest per *25m* only. This data thinning step limits the amount of survey data that has to be processed, and emphasises the most important part of the sea floor for hydrography: its shallowest points. Shoal-biasing does not only affect the accuracy (as indicated in the previous paragraph), but also introduces an artificial uplift: more often, observed depths $\underline{d}$ are chosen that are shallower than the true depth $d$. Because the accuracy $\sigma_d$ indicates that the noise $\underline{e}_d$ is comparable for all surveys, this effect is assumed equal for all surveys. Therefore, these artefacts will not appear in an estimation of dynamics, and are neglected.

Figure 4 is an example of the calculation of the covariance function. The circles are the autocovariances, at specified distances in the specified direction. In fact, a direction interval of *22.5°* was used. Such an interval is necessary to obtain enough data to estimate the autocovariance at this distance. Also, the distance represents in fact a distance interval of the size of the autocovariance spacing. The structure on the sea floor is too irregular to show a repeating pattern in its covariance function in *x*-direction. The negative autocovariances do indicate a wave pattern: a small depth at a certain position corresponds to a high depth half a wavelength further, and vice versa. For small distances, not many pairs of depths are available. Therefore those covariance values may become inaccurate, as visible in the second graph, which is the *y*-direction. Clearly, this area is anisotropic, as the autocovariances in the two directions differ.

For both directions, we fit the gaussian function (2). Such a function cannot be negative, and therefore it does not fit at the end of the first graph. The interpolation is limited to observed positions within a hundred metre square around the node, i.e. the nodal distance. This guarantees that every observation is used only once, and therefore limits the covariance between the nodes to a minimum. Therefore, we should not worry about a bad fit at distances of several of hundreds of metres. The covariance values in the first graph do not show a clear periodicity, and therefore the sand wave version of function (2) is not used. Figure 5 presents the

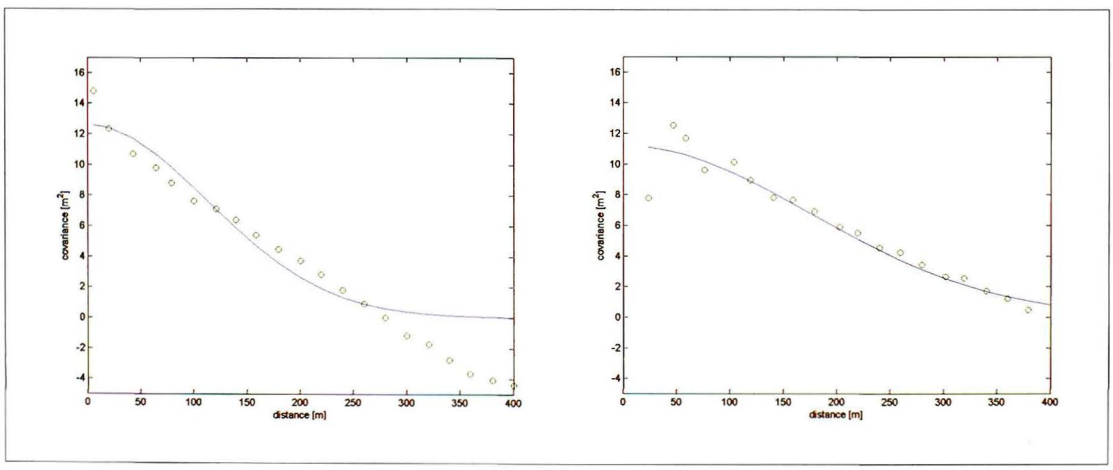


*Figure 4: Covariance functions for the 2003 survey of the Southern part of critical area I. The first graph shows the autocovariances of the sounded depths in the x-direction (circles), which corresponds to the direction of highest variability, and their fitted function. The second graph shows the autocovariances in the perpendicular y-direction as well as their fitted function. The value at distance zero is not shown. It corresponds to the variance, which is a singular point that is equal for both the graphs*

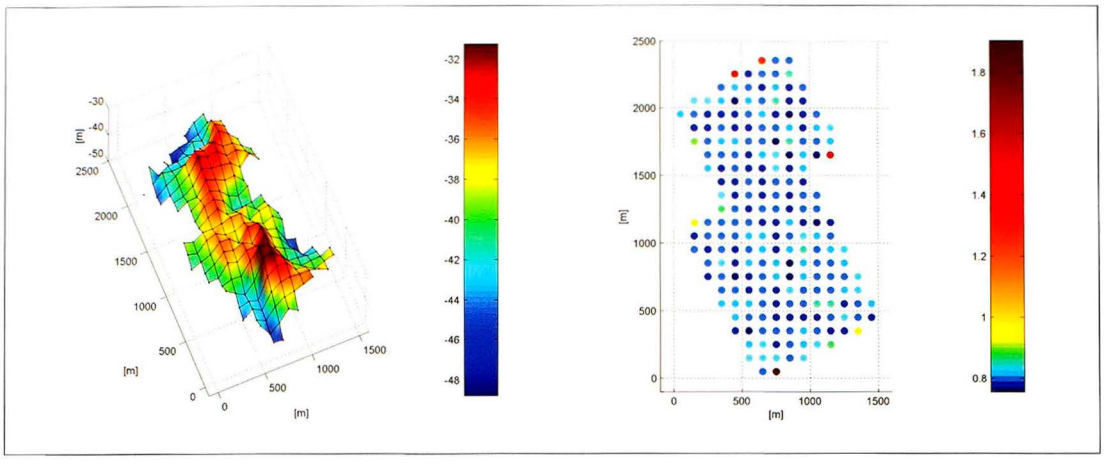


*Figure 5: Gridded depth under the mean lower low water spring level [m], and their accuracies at 95% probability [m], for the 2003 survey of the Southern part of critical area I. The vertical axis of the first graph was exaggerated hundred times. The colour bar of the second graph was modified to show the accuracy differences in the middle of the grid*

results of the kriging process. It is obvious from a comparison with Figure 3 that some nodes at the boundary of the area could not be estimated well, and therefore have a higher standard deviation.

## 5a. Deformation Analysis: The Sea Floor Model

The third step of the method is the application of deformation analysis [Caspary, 1987]. When the depths $d_p$ at grid positions $p$ become available, the observation and interpolation processes have added noise $\underline{e}_d$ and $\underline{e}_i$ to the depths: $\underline{d}_p = d_p + \underline{e}_d + \underline{e}_i$. An area of a shallow sea floor can be modelled by a sloping plane, possibly superimposed by a sand wave pattern [Dorst, 2004a; 2005]. Here, we limit ourselves to the planar analysis, as the geostatistics showed that the area is not suitable for sand wave analysis.

$$d = d_{(0,0)} + x \cdot \alpha_x + y \cdot \alpha_y \quad . \tag{4}$$

We use this expression to relate the depths $\underline{d}_p$ at the positions $(x_p, y_p)$ to the sea floor parameters that describe the modelled sea floor. They are the depth of the grid origin $d_{(0,0)}$ and the planar slopes $a$ in the perpendicular horizontal directions $x$ and $y$.

The sea floor parameters are collected in a vector $x$, and their relations with the observed depths are described in a model matrix $\boldsymbol{A}$, resulting in:

$$\underline{\boldsymbol{d}} = \boldsymbol{A} \cdot \boldsymbol{x} + \underline{\boldsymbol{e}}. \tag{5}$$

$\underline{\boldsymbol{d}}$ is the vector containing all observations $\underline{d}_p$, $\underline{\boldsymbol{e}}$ collects the noise scalars $\underline{e}_p$. The variances $\sigma_p^2$ are collected on the main diagonal of covariance matrix $\boldsymbol{Q}_d$. If it is assumed that the observation noise has a normal distribution $N(0,\sigma_p^2)$, adjustment theory [Teunissen, 2000] states that the Best Linear Unbiased Estimators (BLUE-s) $\hat{\underline{\boldsymbol{x}}}$ of the sea floor parameters can be calculated as the least squares solution.

In general, a model consisting of just a sloping plane, and possibly a sand wave pattern does not describe a piece of the sea floor very well. However, the goal of the method is not to describe the sea floor, but to detect its changes. It will be shown in Dorst [2005] that changes in this model do represent average changes of the depths, slopes and sand wave well, by an artificial dataset. Other artificial examples are already available [Dorst, 2004b; Menting, 2004].

## 5b. Deformation Analysis: Model Extensions

To include the description of sea floor deformations, the model (5) needs to be extended. If depth observations at positions $p$ are available from several surveys, $\underline{\boldsymbol{d}}$ is filled with observation vectors $\underline{\boldsymbol{d}}_p[s]$ instead of single observations $d_p$ for every $p$, where $s$ indicates the survey from which a depth at $p$ was deduced. If the sea floor is static, the vector of sea floor parameters does not change, and model (5) is sufficient. However, if the sea floor is

dynamic, new model parameters that describe these dynamics have to be added to equation (5) [Teunissen, 2001]:

$$\underline{d} = A \cdot x + B_a \cdot \nabla_a + \underline{e}. \qquad (6)$$

$\boldsymbol{B}$ is a matrix that contains the new model parts, and $\nabla$ a vector that contains the new sea floor parameters. Model (5) is now called the null hypothesis $H_0$, and model (6) the alternative hypothesis $H_a$ for model extension $\boldsymbol{B}_a$. An extension consists of both the depth at the origin, and the slopes, as they are not independent: a planar slope change also leads to a change in the depth parameter, except in the improbable case the plane rotates exactly around the grid origin.

This way, model extensions can for instance be formulated for a linear trend, an outlying survey, and general deformation. We call a sea floor change "generally deforming" if differences are too large to be explained by noise, but no trend or deviating survey can be found. In testing theory [Teunissen, 2001], an outlier is a single observation that does not correspond with the others; similarly, a survey that clearly differs is called "outlying" here. Causes can both be a true sea floor change and irregularities in the survey process. The model that describes the dynamics sufficiently well can be solved by the least squares solution.

Now, a choice has to be made which hypothesis, or combination of hypotheses, fits the data best. Testing theory does this by calculating a test statistic $T_a$ for every $H_a$ [Teunissen, 2001]. The value of the test statistic is compared to a critical value $k_\alpha$: $H_0$ is rejected if $T_a$ is larger than $k_\alpha$. – i.e. the differences between surveys are too large to likely be caused by the noise, and therefore indicate sea floor dynamics. However, if $H_0$ is true – i.e. the sea floor is static, still $T_a > k_\alpha$ with $\alpha$% chance, due to the misleading influence of the observation noise. In other words: $\alpha$ is the probability that $H_a$ is accepted if in fact $H_0$ is true; this probability of a 'false alarm' for sea floor dynamics is called the level of significance. A small $\alpha$ is desirable, but it implies a large probability $\beta$ that $H_0$ is accepted if in fact $H_a$ is true, the 'missed alarm'. The optimal choice for $\alpha$, and therefore $k_\alpha$, depends on the risk of a 'false alarm' compared to the risk of a 'missed alarm'.

If several alternative hypotheses are compared to a null hypothesis simultaneously, the one that has the largest quotient $T_a/k_{\alpha,a}$ is accepted as true, if this quotient is larger than one. Hereafter, the model is extended, and the remaining alternative hypotheses are tested again, until the largest quotient is smaller than one. The various hypotheses can be adjusted to each other by tuning the probabilities $\alpha$: a larger percentage corresponds to a smaller value for $k_\alpha$ and thus to a faster acceptance of an alternative hypothesis, and vice versa. Default values for the levels of significance might be chosen as: *10%* for trends, *5%* for general instability and *1%* for outliers, in case of usage for survey plan improvement. A choice reflects the importance that is given to the detection of any kind of deformation. For this application, we considered it very important to detect trends, and not so important to detect single outlying surveys. If deformation analysis would be applied to the processing of a new survey in office, emphasis might for instance be placed on the question if the new survey confirms the previous ones. In that case, the level of significance for detection of outlying surveys should be chosen higher than the level for trend detection [Dorst, 2004b].

| scenario | mdb for an outlying mean depth | mdb for a trend in mean depth |
|---|---|---|
| usual | *1* | *1* |
| half the standard deviations | *1/2* | *1/2* |
| double the number of surveys, original survey frequency | *↑1* | *↓1/4* |
| double the survey frequency, original time interval | *↑1* | *1/√2* |

*Table 2: Factors for the minimal detectable biases for several scenarios. "↑" means 'approaches the value from a smaller one for large numbers of surveys', "↓" means 'approaches the value from a larger one for large numbers of surveys'. For large numbers of surveys, the values behind the arrows will almost be reached, but the exact values are only valid for an imaginary infinite number of surveys*

As we realised in the section on variance propagation, the accuracy might be worse than specified. A worse accuracy leads here to a faster rejection of the null hypothesis, i.e. it is rejected incorrectly more often than indicated by the levels of significance. The real accuracy is worse than assumed, so observation noise will be interpreted as sea floor deformation too often. However, an analysis procedure that warns too often for dynamics is not considered as problematic as the opposite.

### 5c. Deformation Analysis: Minimal Detectable Biases

One might ask: how large should a change in the sea floor be to be detected? This can be answered by calculating minimal detectable biases (mdb-s) [Teunissen, 2001]. Often, the probability $1-\beta$ of detecting a true change with the size of the minimal detectable bias is chosen *80%*. Larger changes can be found more probable, smaller changes less probable.

Table 2 gives an example of the usefulness of minimal detectable biases: they can be applied as a tool to plan surveys. The quality of detecting dynamics for a set of surveys of an area might be given by normalised minimal detectable biases. When it is required to improve the monitoring of this area, several scenarios can be opted for. If it is decided that the survey gear should be replaced by higher quality equipment, the minimal detectable biases indicate that an improvement to half the standard deviation of every sounding of every survey leads to half the size of the dynamics that can be found. A densification of survey lines also has a positive effect on the quality of the grid nodes, and therefore on the size of the mdb-s.

A continuation using the same equipment, while waiting with the analysis until double the number of surveys have been done is hardly worthwhile for outlier detection, but very much so for the estimation of a trend. A doubled survey frequency for the original time interval has the same influence on outlier detection as this number of surveys in any other time interval (one row higher). The doubled frequency gives less improvement on the size of detected trends than the previous scenario. In conclusion, if the mdb-s are smaller than necessary, savings can be made on survey frequency or track spacing, and if they are higher than specified, an investment in survey frequency or equipment should be considered.

### 6a. Results of the Example: Past Deformations

Surveys are available for the years 1991, 1995, 1998, 2000, 2002 and 2003. The calculated nodal depths and their standard deviations of all surveys are comparable. The exception is the 1995 survey, which has a worse accuracy, due to a doubled track spacing. The levels of significance are given their default values, given here above.
The deformation analysis can be applied to this area as a whole, but also to every node individually. In this last case, only the first parameter of expression (2) remains. Table 3 shows that a lot of change will be invisible when analysing per node: only large dynamics can be found with at least *80%* probability. The decrease of the number of used nodes from over two hundred to one introduces a change of an order of magnitude to the mdb-s. Typical accuracies at *95%* level are *0.1m/year* for a trend, and *1.0m* for an outlier. The advantage of the node-by-node approach is the indication of what is happening inside an area: resolution is gained, but accuracy is lost. Therefore the combination of nodal analysis and area analysis gives an optimal insight into the dynamics of an area. E.g., a nodal analysis can be used to define the areas for the area analyses.

| type of analysis | mdb-s for outlying mean depth [m] | mdb-s for trend in mean depth [m/yr] |
|---|---|---|
| per node | 1.50 | 0.12 |
| per area | 0.12 | 0.01 |

*Table 3: Minimal detectable biases that can be detected with 80% probability for the six surveys of the Southern part of critical area I, for levels of significance of 10% for trends and 1% for outliers*

Figure 6 visualises the outcome of the nodal analysis. An interesting behaviour of the crest was found: many nodes at the left side subside, and so do nodes at the backside. But, some rising and other behaviour is visible as well. The trough at the right is more static. A node is static if the null hypothesis is accepted; i.e. all differences between depths can be

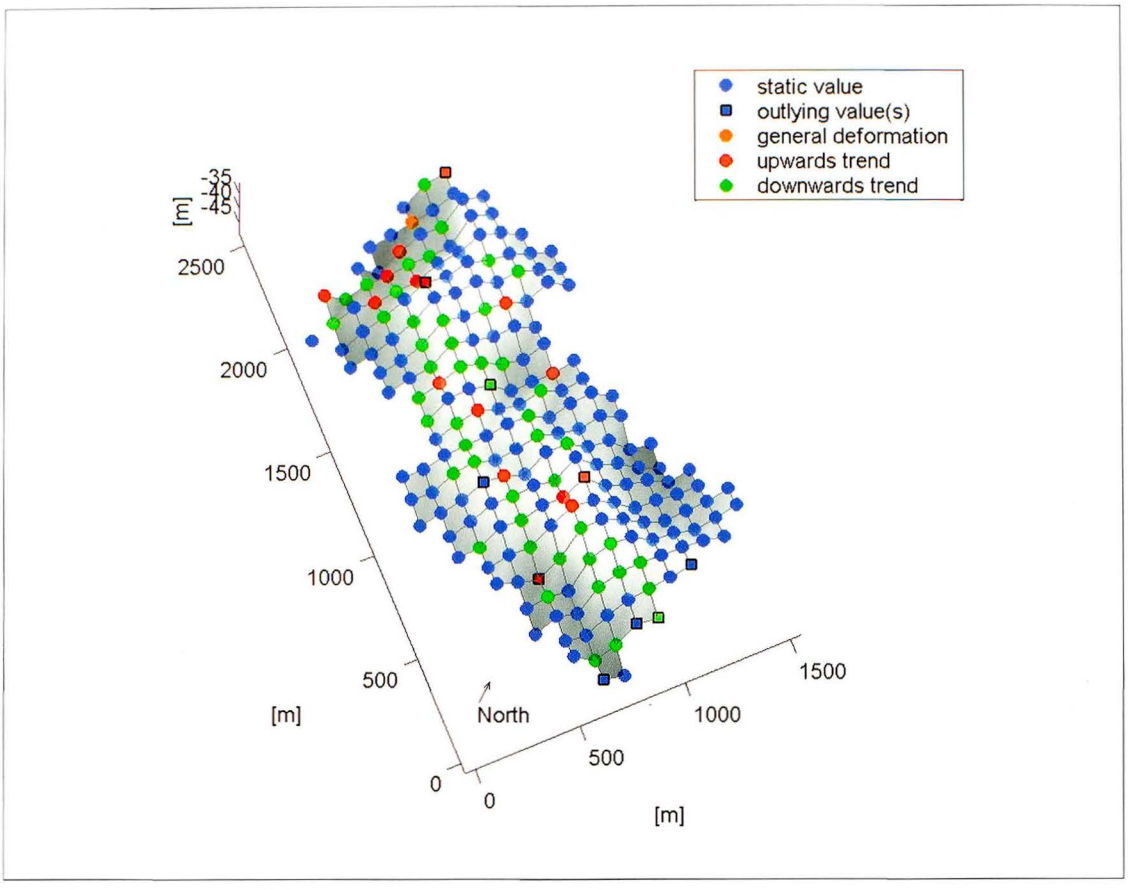


*Figure 6: Results of the nodal analysis of the Southern part of critical area I. The grid is shown horizontally, the vertical axis shows depth. The intensity of the colours shows the size of the dynamics. The maximum dynamics are: upwards speed 0.13m/year at (550; 550); downwards speed 0.17m/year at (650; 550); 0.69m standard deviation for general instability at (650; 2250); and an outlier of 5.80m at (950; 150). The vertical axis was exaggerated hundred times*

explained by the size of the observation noise. Remember that the levels of significance indicate that one out of every ten detected trends is artificial, as is one out of every hundred outliers.

The more accurate area analysis shows in Figure 7 that several model extensions were necessary to model the dynamics of this area: a trend (in green), and three surveys that did not fit well into this trend, and thus were identified as outliers (in grey). In other words, average differences between surveys appeared to be larger than could have been expected from the inaccuracies of the grid depths. The first graph of Figure 7 shows that the modelled trend was small and downward. The other surveys deviate up to several decimetres. Of course, the true average deformations of the area are more complicated. The given solution is the best approximation of the dynamics given the specified hypotheses. A larger set of hypotheses will improve the description of the deformations. If we decide to use linearised sea floor models, non-linear hypotheses could be specified as well.

The changing slopes of the estimated plane are shown in the second and third graph. They are not very relevant, as indicated by the size of their evolution with respect to the accuracy intervals. Their evolution shows that the dynamics are not exactly the same for all parts of the area. It is clear from the three graphs that the model behaviour of the depths and the slopes are dependent: the same model extensions are used in all the graphs, because planar movement as a whole is modelled in the alternative hypotheses.

Note the behaviour of the accuracy intervals of Figure 7: in general, an outlying parameter value can-

not be estimated as well as the other values. Values in a trend can be estimated best if they are in the middle of the time interval. The worse grid accuracy of the 1995 survey causes the large accuracy interval of the second survey.

## 6b. Results of the Example: Predictions

An application of the node analysis results is the deduction of an advised moment to survey the area again. Hereto, a prediction of the depths should be made on the basis of the calculated dynamics of every node. Of course, such extrapolation is very risky: it assumes that the observed dynamics in the past still continue in the future. It is therefore not a good idea to actually use the predicted depths.

The graphs of Figure 8 confirm the decreasing quality of the predictions with time. They show the accuracies of predictions zero and ten years ahead. We call a prediction to the moment of the latest survey a null-prediction. The standard deviations are growing in time at nodes where a trend has been detected. Nodes that show outlying values, or a general deformation, have larger standard deviations than static nodes. However, these kinds of nodes do not show a worse accuracy with time, as their modelled behaviour is time-independent. It is important to realise that these prediction results are only valid in the context of the accepted models for every node. In reality, of course, the uncertainty of the prediction of every node grows with time. The method of Wüst [2004] produces such growing accuracies, and therefore predicts more realistically.

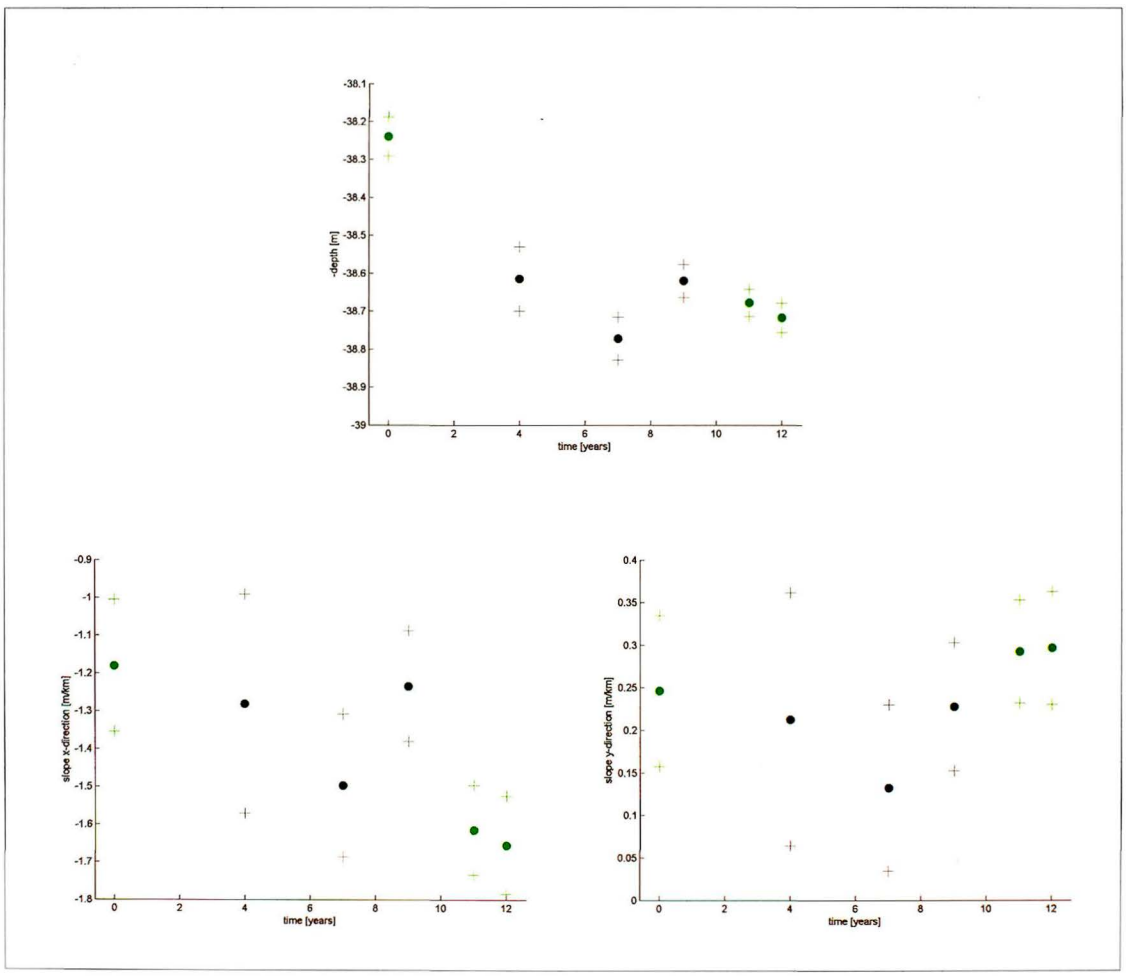


*Figure 7: Results of area analysis (dots), and their 95% accuracy intervals (plusses), for the Southern part of critical area I. Years since the first survey, in 1991. For the first graph, the origin of the grid was shifted to the middle of the area. This way, the shown depths equal the accuracy-weighted mean depths*

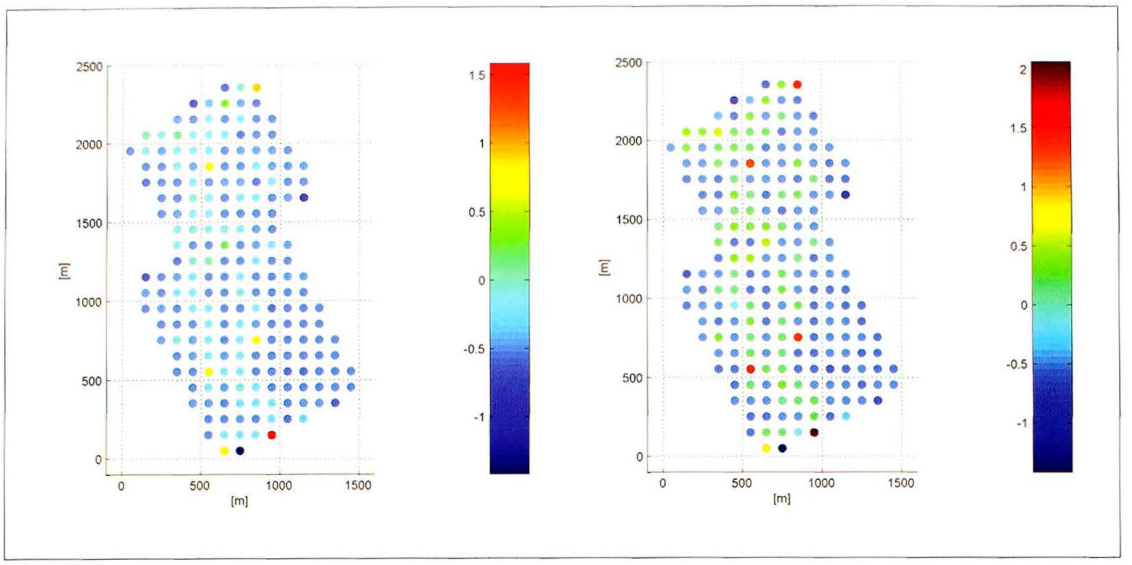


*Figure 8: Change in accuracy, at 95% level [m] with respect to the 2003 survey (Figure 5, second graph), for predictions zero and ten years ahead, for the grid of the Southern part of critical area I*

The accuracies in Figure 8 are relative to those for the latest survey, shown in Figure 5. It may be a surprise to see that many predictions give more accurate results than a single survey. It can be concluded from this figure that the observation and interpolation noise of most of the nodes of the 2003 survey can be decreased by including information of past surveys. For nodes that show a trend, the standard deviations can be smaller than those of the latest survey for two reasons. This happens if this node was not known accurately from the latest survey, or if the trend is small. For static nodes, every survey shows an image of the sea floor that is just as current as the others. The null-prediction then simplifies to an accuracy-weighted average of the surveys, what seems to be the most logical choice, and it is the most accurate solution as well. Again, these considerations are only valid within the context of the accepted combination of hypotheses.

These rather unreal accuracies can be used very well as a tool to decide whether a new survey is already necessary: when too many grid nodes have a too large variance, it is time to survey again. Larger modelled dynamics mean higher resulting inaccuracies, especially larger trends mean they grow faster. Further, when fewer surveys have been conducted in an area, larger predicted inaccuracies occur. For instance, the IHO S44-standards for bathymetry model accuracy can be compared to the predicted standard deviations [International Hydrographic Organization, 1998]. In the example, the inaccuracies hardly grow, because there are already many surveys available, and the dynamics are often small, or absent. Both facts may support a decision to postpone a next survey here. Other uses of these predictions than survey plan improvement should not be advised.

## 7. Discussion

The example of application of deformation analysis to the sea floor shows that the method enables the precise estimation of average dynamics of an area, and a rough estimation of dynamics within this area. Those two analysis scales support each other: one cares for the resolution, the other for a precise estimation of average behaviour. It is a good idea to analyse on intermediate scales as well. However, it should be cared for that only those parts of the sea floor are grouped together into an area that show equal spatial variability and temporal dynamics. Therefore, large areas should be analysed piece-wise.
We have seen that, although a wavelike structure was present in the analysed area, it was too irregular to model sand wave dynamics.

An advantage of the presented method is that it only needs the archived surveys and their meta data. It

is not necessary to obtain information about the circumstances in the area during the analysis period: weather, human activities, et cetera. However, if it is known that a specific kind of deformation may have happened, this could be tested by specifying appropriate alternative hypotheses. On the other hand, if a temporary anomaly has been present, the limited temporal resolution of the surveys may cause that it is missed: it is not possible to extract information that is not inside the surveys. Therefore, it is very important to use the results only as one aspect of a decision about survey priority. Such a decision should also be based on the local circumstances, and other approaches to the estimation of dynamics of an area, like the physical modelling of sea floor dynamics [Nemeth et al., 2002; Roos and Hulscher, 2003].

The detection of dynamics depends to a large extend on the variance of the depths. However, it is hard to find good values for their accuracy. In this example, *a priori* values were calculated by the propagation of all stochastic aspects of the measurement and interpolation process. An easier but possibly too optimistic approach is the use of *a posteriori* values by binning observations. Detection of dynamics and their kind depend on the choice for the levels of significance. They can be adjusted for the specific purpose of the analysis: is detection of trends in the sea floor behaviour the most important, or maybe the detection of outlying surveys? Good choices for the accuracy of depths and the levels of significance only come with experience. As the detection of dynamics depends completely on those choices, a wrong choice may lead to improbable analysis results. This is another reason to use deformation analysis only as one of the several influences on a decision on survey planning.

The observation and interpolation noise is thought of as being uncorrelated: the influence of stochastic deviations on one nodal depth is then independent of their influence on other nodal depths. In practice, this is not the case: e.g. errors due to tidal reduction are correlated in time, and unnoticed variations in the speed of sound through water are temporally and spatially correlated. The covariances between the gridded depths, that have a place in the depth covariance matrix $Q_d$, have been neglected for simplicity. The size of this neglected correlation and its effect on the analysis results have not been studied yet.

Detected dynamics can always be due to two causes: a sea floor deformation and a bias in the surveys. Deformation analysis does not take this decision: it only shows if surveys confirm each other, and how the differences behave. The analyst should interpret the cause of differences. Especially in case of a single outlying survey, it is hard to decide whether malfunctioning of equipment has caused an artefact, or that a real sea floor disturbance has happened.

## 8. Conclusion

The presented method has shown to be a valuable aid in the planning phase of the survey process for the Hydrographic Service of the Royal Netherlands Navy. The usage of minimal detectable biases could improve a survey plan, to reach a better equilibrium between accuracy and cost. The standard deviations of predictions per node could help to find an acceptable survey moment. Most importantly, the combined estimation of dynamics per node and per area could support decisions about survey priority.

The shown critical area does not show large dynamics. None of the other critical areas has larger dynamics either. The Hydrographic Service considers surveying the critical areas less frequently now.

## References

Calder, B. (2003), *Automatic statistical processing of multibeam echosounder data*, Int. Hydro. Review, New Series 4(1), 53-68

Caspary, W.F. (1987), *Concepts of Network and Deformation Analysis*, Monograph 11. Kensington, Australia: University of New South Wales, School of Surveying

Chilès, J.-P., and P. Delfiner (1999), *Geostatistics, modeling spatial uncertainty*. New York: John Wiley & Sons

Cressie, N., and J. Kornak (2003), *Spatial statistics in the presence of location error with an application to remote sensing of the environment*, Statistical Science, 18(4), 436-456

Deutsch, C.V., and A.G. Journel (1992), GSLIB: *Geostatistical Software Library and User's Guide*. Oxford, UK: Oxford University Press

Dorst, L.L. (2004a), *Geodetic deformation' analysis: a new method for the estimation of seabed dynamics*. In: Hulscher, S.J.M.H., T. Garlan, and D.Idier (eds.), Proc. MARID2004, 2nd international workshop on Marine Sandwave and River Dune Dynamics, Enschede, The Netherlands, 64-71

Dorst, L.L. (2004b), *More efficient and reliable sea floor mapping by geodetic interpretation of bathymetric data*. Proc. ECUA2004, 7th European Conference on Underwater Acoustics, Delft, The Netherlands

Dorst, L.L. (submitted for publication in 2005), *A statistical method for the detection of sea floor dynamics in depth data*, J. Geophys. Res.-Earth Surface

Elema, I.A. and M.C. Kwanten (1999), *Determining Squat for the Hydrographic Vessels of the Royal Netherlands Navy using GPS-OTF Techniques*, The Hydrographic Journal, July 93, 3-7

Hulscher, S.J.M.H., and G.M. van den Brink (2001), *Comparison between predicted and observed sand waves and sand banks in the North Sea*, J. Geophys. Res., 106(C5), 9327-9338

Hydrographic Department (1990), *The Assessment of the Precision of Soundings*. Professional paper no. 25. London: Ministry of Defense (Navy)

International Hydrographic Organization (1998), *IHO Standards for Hydrographic Surveys*. Special publication no. 44, 4th edition. Monaco: International Hydrographic Bureau

Kielland, P., and M. Dagbert (1992), *The use of spatial statistics in hydrography*, Int. Hydro. Review, 69(1), 71-92

Knaapen, M.A.F., and S.J.M.H. Hulscher (2002), *Regeneration of sand waves after dredging*, Coastal Engineering, 46, 277-289

Knaapen, M.A.F., S.J.M.H. Hulscher and H.J. de Vriend (2001), *A new type of sea bed waves*, Geophysical Research Letters, 28(7), 1323-1326

Marcotte, D. (1991), *Cokrigeage with Matlab*, Computers & Geosciences, 17(9), 1265-1280

Menting, P.G. (2004), *Predicting sea floor changes in the North Sea*, Graduation report of the Delft University of Technology

Nemeth, A.A., S.J.M.H. Hulscher and H.J. de Vriend (2002), *Modelling sand wave migration in shallow shelf seas*, Continental Shelf Research, 22, 2795-2806

RIKZ (1997), *Gebruikershandleiding DIGIPOL*, Rijkswaterstaat, Rijksinstituut voor Kust en Zee

Roos, P.C., and S.J.M.H.Hulscher (2003), *Large-scale seabed dynamics in offshore morphology: modelling human intervention*, Rev. Geophys., 41(2), 5/1-5/19

Schaap, J. (2000), *Hydrografisch werk op de Noordzee*, Marineblad, 100(7/8), 237-242

Sieben, J. (2004), *Characterization of bed levels with statistical equivalency*. In: Hulscher, S.J.M.H., T. Garlan, and D.Idier (eds.), Proc. MARID2004, 2nd international workshop on Marine Sandwave and River Dune Dynamics, Enschede, The Netherlands, 276-283

Smith, Lt. S.M., Dr. L. Alexander and Capt. A.A. Armstrong (2002), *The navigation surface: a new database approach to creating multiple products from high-density surveys*. Int. Hydro. Review, New Series 3(2), 12-26

Teunissen, P.J.G. (2000), *Adjustment theory; an introduction. Series on Mathematical Geodesy and Positioning, Delft, The Netherlands: Delft University Press*

*Teunissen, P.J.G. (2001), Testing theory; an introduction*. Series on Mathematical Geodesy and Positioning, Delft, The Netherlands: Delft University Press

Velberg, P.J. (1993), *The accuracy of the depth information of the nautical chart*, The Hydro. Journal, 68, March 1993, 29-35

Versteeg, H.A. (2000), *Tidal Reduction on Fairsheet Level: A modern approach to on-board prediction of water levels*, Hydro INTERNATIONAL, 4(7), 6-9

Wells, D.E., and D. Monahan (2002), *IHO S44 standards for hydrographic surveys and the variety of requirements for bathymetric data*, The Hydro. Journal, 104, April 2002, 9-15

Wright, P., (1992), *Long term changes to the positions and heights of sand waves in the Southern North Sea*, Int. Hydro. Review, 69(2), 113-128

Wüst, J.C. (2004), *Data-driven probabilistic predicitions of sand wave bathymetry*. In: Hulscher, S.J.M.H., T. Garlan, and D.Idier (eds.), Proc. MARID2004, 2nd international workshop on Marine Sandwave and River Dune Dynamics, Enschede, The Netherlands, 338-345

## Acknowledgements

The author has the pleasure to acknowledge: his colleagues at the Hydrographic Service, for giving direction to this project, especially Ina Elema and Jan Appelman; Suzanne Hulscher and Pieter Roos, at the University of Twente, for their valuable advises; Yves Gratton, at the University of Quebec, for sharing the Kriging toolbox.

## Biography

Leendert Dorst finished his MSc in Geodetic Engineering at the Delft University of Technology in 1999. His final research project was the analysis of a time series of gravimeter data at the Royal Observatory of Belgium, using wavelets. Since 2000, he has been employed at the Netherlands Hydrographic Service, where he works on maritime positioning, technical aspects of the law of the sea, and the analysis of time series of survey data. Recently, he started a PhD project on the last subject at the University of Twente.

E-mail: ll.dorst@mindef.nl